JOURNAL OF SOLID STATE CHEMISTRY 69, 299–311 (1987)

# Polymorphism of the Bivalent Metal Vanadates $MeV_2O_6$ (*Me* = Mg, Ca, Mn, Co, Ni, Cu, Zn, Cd)

KRZYSZTOF MOCAŁA AND JACEK ZIÓŁKOWSKI*

*Institute of Catalysis and Surface Chemistry, Polish Academy of Sciences, 30-239 Kraków, ul. Niezapominajek, Poland*

Received June 9, 1986; in revised form November 24, 1986

Based on the literature data, our former findings and additional DTA and high-temperature X-ray studies performed for $CdV_2O_6$, $MgV_2O_6$, and $MnV_2O_6$, a consistent scheme of the phase transformations of the $MeV_2O_6$ (*Me* = Mg, Ca, Mn, Co, Ni, Cu, Zn, Cd) metavanadates is constructed at normal pressure between room temperature and melting points. Three types of structures exist for the considered compounds: brannerite type (B), pseudobrannerite type (P), and $NiV_2O_6$ type (N). The following phase transformations have been observed: *Me* = Mg, B → P at 535°C; *Me* = Mn, B → P at 540°C; *Me* = Co, N → B at 660°C; *Me* = Cu, B (with triclinic distortion) → B at 625°C (secondary order); and *Me* = Cd, B → P at 170°. $CaV_2O_6$-P, $NiV_2O_6$-N, and $ZnV_2O_6$-B exist in unique form in the entire temperature range. P-form seems to be favored by *Me* of larger ionic radii. N-form seems to appear at a peculiar *d*-shell structure and small *Me* size. Preliminary explanation of the dependence of the structure type on *Me* size is offered. New X-ray data are given for $CdV_2O_6$-B, $CdV_2O_6$-P, $MgV_2O_6$-B, $MgV_2O_6$-P, and $MnV_2O_6$-P. 

## Introduction: Evaluation of Literature Data

Among the bivalent metal vanadates $MeV_2O_6$ (*Me* = Mg, Ca, Mn, Co, Ni, Cu, Zn, Cd, Hg), four different structures are known. These are columbite type (C), brannerite type (B), pseudobrannerite type (P) (so called in this paper because of the high analogy to the brannerite), and $NiV_2O_6$ type (N). Depending on temperature and pressure, $MeV_2O_6$ compounds show a polymorphism, though not all of the above-mentioned structures are known for all of the listed *Me*. A minor exception is $CuV_2O_6$, which in the "columbite" and in the low-temperature "brannerite" modifications exhibits a slight monoclinic or triclinic distortion, respectively, ascribed to the Jahn–Teller effect (*1–3*).

As widely reported by Gondrand *et al.* (*1*), orthorombic columbite-type structures (*Me* = Mg, Mn, Co, Ni, Cu, Zn, Cd) exist at high pressures. We shall refer to this paper only to compare the structures, and we intend to concentrate our attention on all other, normal-pressure modifications, stable between room temperature and the respective melting points.

Monoclinic, brannerite-type structures are known for *Me* = Mg (*4*), Mn (*1, 5*), Co (*6, 7*), Cu (*3, 8*), Zn (*9, 10*), Cd (*11*), and Mg (*9*). In this structure originating from $ThTi_2O_6$ (*12*) both *Me* and V are octahedrally coordinated to oxygen. As seen in Fig. 1a, $VO_6$ octahedra linked by three

* To whom all correspondence should be addressed.



0022-4596/87 $3.00

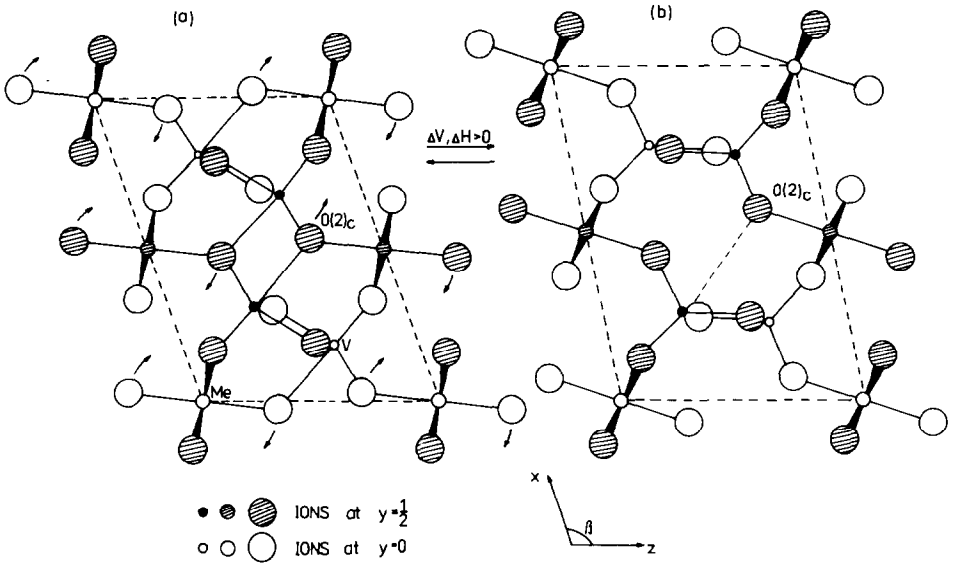


FIG. 1. Brannerite-type (a) and pseudobrannerite-type (b) structures and a scheme of movement of ions during the phase transformation.

edges form the infinite anionic layers parallel to (001); inside the layers zigzag $(VO_6)_n$ chains may be distinguished along [010]. $MeO_6$ octahedra joined by opposite edges form the infinite rows along the *b* axis and link the anionic layers. As one of the V–O bonds is much longer than the others, the coordination of V is frequently labelled as 5 + 1. The transition from the brannerite to columbite-type structure (*1*) involves an increase of vanadium coordination from 5 + 1 to 6, a change in oxygen packing from cubic to hexagonal close-packed, a retention of a part of the structure of the $VO_6$ sheets, and a collapse of the $MeO_6$ rutilelike chains into $PbO_2$ chains. As a result the structure becomes more compact (which is usually the case with high-pressure modifications) and the density of columbites is 6–10% higher as compared with brannerites.

On the contrary, the brannerite → pseudobrannerite transformation described so far solely for $CdV_2O_6$ (*11*, *13*) is followed by the increase of the unit cell volume of about 12%. Simultaneously the parameters *a*, *b*, and *c* grow by 4.65, 1.34, and 0.54%, respectively, and the $\beta$ angle decreases from 112 (a value of 110–112° is characteristic for all other B-type phases) to 103.76°. The B → P transformation may be described (Fig. 1) as a result of "rotation" of $(VO_6)_n$ zigzag chains around the *b* axis, so that one of the oxygens $O(2)_c$ moves away from vanadium (V–O distance increases from 2.6 to 3.6 Å) and the coordination of the latter becomes trigonal bipyramid $VO_5$. In this way $(VO_6)_n$ chains belonging to the infinite (001) anionic layers in brannerite transform in pseudobrannerite into the isolated $(VO_5)_n$ chains. Pseudobrannerite-type structure is also known for $CaV_2O_6$ (*14*).

The structure of $NiV_2O_6$ has never been resolved. Only a nonindexed X-ray pattern is known (*15*). One of the $CoV_2O_6$ modifications has the same structure (*7*, *15*).

According to the literature there are three $MeV_2O_6$ compounds crystallizing at normal pressure and above room temperature in only one modification; these are $CaV_2O_6$-P (*14*), $NiV_2O_6$-N (*15*, *16*), and

$ZnV_2O_6$-B (*16, 17*).[1] Their melting points are 761, 747, and 645°C, respectively.

$CoV_2O_6$ has the N-type structure below 660°C, transforms into B above this temperature, and melt at 740°C (*7, 16*). It may be worth recalling after (*7*) that (1°) B → N transformation is strongly hindered and $CoV_2O_6$-B, quenched to room temperature, may exist in this form for a long time (several months) and (2°) a small admixture of molybdenum, leading to the formation of solid solution $Co_{1-x}Ø_xV_{2-2x}Mo_{2x}O_6$ (Ø = cation vacancy, $0.02 \leq x \leq 0.20$), stabilizes B-type structure until room temperature.

$CuV_2O_6$ at room temperature shows a little triclinic distortion (Bt) from the typical B-type structure. With increasing temperature the distortion fluently diminishes, at 625°C we deal with a secondary-order transformation to B, and at 642°C the compound melts (*2, 3*).

$MnV_2O_6$ has B-type structure up to 540°C. The structure of the high-temperature modification is unknown. Manganese metavanadate melts incongruently at 825°C (*5, 16, 19*).

According to Bouloux *et al.* (*11, 13*), $CdV_2O_6$ is of P-type below 670°C and of B-type above this temperature until the melting point at 800°C. At 670°C a small endothermal effect was observed in DTA, proving that $\Delta H > 0$. This P → B phase transformation is described as a rare one, accompanied by contraction taking place at high temperature. The unusual behavior of $CdV_2O_6$ has been proved in the following way. According to the Clausius–Clapeyron equation

$$\frac{dp}{dT} = \frac{\Delta H}{T\Delta H}. \tag{1}$$

As $\Delta H < 0$ and $\Delta V < 0$, the negative $dp/dT$ slope is expected for phase boundary, which means that the temperature of the B → P transformation should diminish with an increase of pressure. It has been observed in fact (*13*) that this temperature is only 460°C under the pressure of 3000 bars.

Recently, Garcia-Clavel *et al.* (*20*) have managed to obtain pure $CdV_2O_6$ as a product of the reaction between CdO and $V_2O_5$ carried out at room temperature and at normal pressure, in atmosphere saturated with water vapor, during a number of days. In the first stage of the synthesis only P modification was formed, but after 12 days the sample exhibited the presence of a small amount of B-phase, the content of which increased with time (up to 60 days when the experiment was stopped). The same authors (*21*) have reported that a pure B-phase was formed when the reaction was carried out at 150°C for 24 hr, conserving all other conditions of the synthesis. Although the quoted authors accept the sequence of the stable phases claimed by Bouloux *et al.* (*13*), their results suggest rather that B-modification is stable at low temperatures. Formation of P before B in the early stages of the reaction at room temperature may be easily explained with the newly formulated, empirical Ostwald rule (*22*), namely: if the synthesized product has various polymorphic modifications, that of the larger molar volume is formed at the beginning. On the other hand, if a reaction mixture is kept in the same conditions for a prolonged time, a metastable product may be formed as the first one and then transformed into the stable phase, but not conversely. Obviously we have to take into account that some experiments were done in air or oxygen (*11, 13*) and others in the presence of water va-

[1] The polymorphs of all discussed $MeV_2O_6$ compounds have the traditional symbols $\alpha$, $\beta$, and $\gamma$. There is, however, no simple relation between these symbols and the types of structures (B, P, or N). Therefore in this paper we shall use, for clarity, the notation $MeV_2O_6$-$X$, where $X$ indicates the structure. Traditional symbols are recalled and compared with the present ones in Fig. 3. As shown in (*18*), $CaV_2O_6$ undergoes a diffuse phase transformation at −13°C, however, no precise structural data are known for the low-temperature modification.

por (*20, 21*) and therefore the sequence of stable phases requires further verification.

Also $MgV_2O_6$ is known to have two polymorphic modifications with transition temperature at 550–570°C (*4, 23–25*), one of them being of B-type (*4*) and the other of questionable structure. According to Slobodin *et al.* (*24*), B-phase is stable at low temperatures, while Palanna (*25*) is convinced that at 560°C (on heating) we deal with P → B transformation. It should be mentioned, however, that (1°) the initial sample of Palanna was reduced and had a hypothetical formula $Mg^{2+}V^{5+}_{2-2x}V^{4+}_{2x}O_{6-x}$, (2°) in both works (*24, 25*) the X-ray patterns were nonindexed, and (3°) the X-ray patterns of the nonbrannerite phases published in (*24, 25*) do not overlap entirely.

As reviewed earlier, a number of $MeV_2O_6$ phases have been identified as belonging to the brannerite or pseudobrannerite types. Although the structure types are inarguable, the ascription of the space group is less clear and some authors hesitate between *C*2, *Cm*, and *C*2/*m*. On the basis of the least-squares method, Bouloux *et al.* (*13*) ascribed $CaV_2O_6$-P, $CdV_2O_6$-P, and $CdV_2O_6$-B to *C*2/*m*. $MgV_2O_6$-B (*4*) and $CoV_2O_6$-B (*6*) have been tentatively ascribed to the same space group but no unequivocal proof has been offered. According to Angenault and Rimsky (*10*), $ZnV_2O_6$-B belongs to *C*2. The difference between *C*2/*m* and *C*2 consists in the fact that atoms are localized either exactly at $y = 0$ and $y = 0.5$ or at $y$ slightly different from these numbers. This influences in particular the symmetry of octahedra. For example, in the case of $ZnV_2O_6$, $ZnO_6$ octahedron is so deformed that coordination of zinc is rather tetrahedral with two more additional distant oxygens.

The aim of the present work is to clear up the problems concerning the polymorphism of $CdV_2O_6$, $MgV_2O_6$, and $MnV_2O_6$ and to construct a consistent scheme of the polymorphic transformations of the $MeV_2O_6$ compounds at normal pressure.

## Experimental

$MnV_2O_6$ was obtained by solid-state reaction between $Mn_2O_3$ and $V_2O_5$ as described in (*5*). $CdV_2O_6$ was synthesized by calcination of the 1 : 1 mixture of CdO and $V_2O_5$ at 600°C for 20 hr, 650°C for 40 hr, and 700°C for 40 hr in air. A part of this sample was melted under an oxygen flow of 70 ml/min (830°C for 3 hr), crystallized on slow cooling (3°C/hr) to 750°C, and quenched to room temperature. $MgV_2O_6$ was obtained by the amorphous precursor method described in detail in (*19*). $Mg(NO_3)_2 \cdot 6H_2O$ and $NH_4VO_3$ were used as substrates and the obtained glasslike intermediate was annealed in air at 520°C for 20 hr and 580°C for 40 hr.

X-ray diffraction patterns were recorded with a DRON-2 diffractometer using $CuK_\alpha$ (for $CdV_2O_6$) and $CrK_\alpha$ ($MgV_2O_6$, $MnV_2O_6$) radiation. For the high-temperature measurements a GPWT-1500 heating stage was applied, controlled within ±0.5°C with a Pt/PtRh thermocouple. The cell parameters were refined with the respective computer program involving the least-squares method (*5*). The phase identification was based upon the published patterns: nonbrannerite $\beta$-$MnV_2O_6$ (*5*) and both P and B or $\alpha$- and $\beta$-$CdV_2O_6$ (*11*). In the case of B-type $\alpha$-$MgV_2O_6$ the powder pattern was calculated from the single-crystal data (*4*).

In this paper, new indexed X-ray patterns for several phases are determined and listed in Tables II and III, including the intensities of reflections. Similarly to $CoV_2O_6$ (*7*), it has been observed that the grains of the studied samples orient easily. Therefore we were not able to obtain quantitatively reproducible intensity data even when using a special technique of preparing an unoriented sample (*5*), which was success-

ful with Mn-containing brannerite-type phases.

DTA curves were recorded with the Setaram M5 Microanalyser at a heating rate of 7°C/min in air or in a stream of oxygen (30 ml/min) using Pt crucibles and $Al_2O_3$ preheated at 1500°C for 24 hr as a reference. The onset temperatures, obtained with the tangent method, were taken as transformation temperatures, the accuracy being ±3°C.

The density of $CdV_2O_6$-B was determined with the modified Jeanning's method (*26*), allowing one to reach an accuracy better than ±0.1%.

## Results and Discussion

### (*i*) $CdV_2O_6$

X-ray phase analysis of our air-synthesized $CdV_2O_6$ preparation performed at room temperature proved that it was pure B-type phase. The determined parameters of the unit cell (Table I) are practically the same as those published by Bouloux *et al.* (*11, 13*), but we seem to have obtained higher precision. $CdV_2O_6$-B was then submitted to X-ray studies in a high-temperature camera, performed in such a way that the sample was heated at a rate of about 10°C/min until a chosen temperature, which was stabilized for about 30–40 min to take the pattern and then the heating was continued. No phase transformation has been observed below 170°C. Because of the thermal expansion, the unit cell parameters determined at 160°C (Table I) are slightly changed as compared to those found at room temperature. Above 170°C the reflections from $CdV_2O_6$-P appear and at 200°C the phase transformation has been completed in a few minutes. All observed reflections could be indexed according to (*11*) as belonging to $CdV_2O_6$-P and the unit cell parameters determined at 250°C are in-

TABLE I

UNIT CELL DIMENSIONS FOR $CdV_2O_6$-B AND $CdV_2O_6$-P[a]

| | $CdV_2O_6$-B | | | $CdV_2O_6$-P | | $\Delta p$ (%)[b] | |
|---|---|---|---|---|---|---|---|
| | Present work | From (*13*) | Present work | From (*13*) | Present work | Based on (*13*)[c] | Present work[d] |
| $T$ (°C) | 20 | r.t. | 160 | r.t. | 250 | | |
| $a$ (Å) | 9.3632(13)[e] | 9.359 | 9.386(4) | 9.794 | 9.837(4) | 4.65 | 4.8 |
| $b$ (Å) | 3.5662(8) | 3.568 | 3.570(1) | 3.616 | 3.618(1) | 1.34 | 1.3 |
| $c$ (Å) | 6.9501(11) | 6.980 | 6.968(3) | 7.018 | 7.020(4) | 0.54 | 0.7 |
| $\beta$ (deg) | 112.13(1) | 112.0 | 111.86(3) | 103.76 | 103.58(2) | −7.36 | −7.4 |
| $c \sin \beta$ (Å) | 6.4381(12) | 6.472 | 6.467(3) | 6.817 | 6.824(4) | 5.33 | 5.5 |
| $V$ (Å$^3$) | 214.97 | 216 | 216.71 | 242 | 242.46 | 12.25 | 12.1 |
| $Z$ | 2 | 2 | 2 | 2 | 2 | | |
| $d_{exp}$ (g cm$^{-3}$) | 4.797 | 4.66 | | 4.28 | | | |
| $d_{x\text{-ray}}$ (g cm$^{-3}$) | 4.793 | 4.77 | | 4.27 | | | |

[a] Systematic absences of reflections $h + k = 2n + 1$ were observed for both modifications.

[b] $p$ is the general symbol of the cell parameters; lower indices indicate the structure and temperature.

[c] $\Delta p = \dfrac{p_{P,\,r.t.} - p_{B,\,r.t.}}{p_{B,\,r.t.}} \times 100.$

[d] $\Delta p = \dfrac{p_{P,\,260} - p_{B,\,160}}{p_{B,\,160}} \times 100.$

[e] Estimated standard deviation in parentheses.

cluded in Table I. They are close to those reported in (*11*, *13*). Further heating of $CdV_2O_6$-P up to 770°C and maintaining at this temperature for 7 hr did not bring about any phase transformation. On cooling, the above-described phase transformation at about 170°C appeared to be reversible with a hysteresis, so that P → B transition was completed in a reasonable time only at 80°C. Because of the explosive character of the P → B transformation, the last-mentioned experiment was done on a sample covered with beryllium foil. The transformation may be visually observed when $CdV_2O_6$-P powder is taken from a furnace (preheated above 170°C) and spread on a glass plate: the grains jump up on cooling.

In agreement with the results of the X-ray studies the $CdV_2O_6$ sample showed in DTA (20–770°C) only one, reversible peak (Fig. 2). On heating, it was endothermal, narrow, and appeared at 172°C. On cooling, it was exothermal, broad, and shifted to 46°C. The areas of both effects were equal with precision of 1.5%.

As the sample studied by Bouloux *et al.* (*11*) was synthesized in oxygen, we have performed analogous X-ray and DTA experiments using the sample of $CdV_2O_6$ prepared by crystallization from the melt under oxygen. The results were essentially the same as described above with two minor differences. Oxygen-synthesized $CdV_2O_6$ showed (1°) one weak, nonidentified additional reflection corresponding to $d$ = 2.734 Å (at room temperature) and (2°) a double endothermal effect between 620 and 650°C (Fig. 2b). It may be supposed that this way of preparation (melting/oxygen) results in a deviation from stoichiometry. It seems worth recalling that a eutectic has been reported in the $CdV_2O_6$–$V_2O_5$ system (*9*), melting at 670°C.

The experiments described above clearly demonstrate that $CdV_2O_6$ is of B-type below 170°C and of P-type above this temperature. There is no contradiction between this conclusion and the high-pressure experiment (*13*) mentioned in the Introduction, as now, for the B → P transformation,

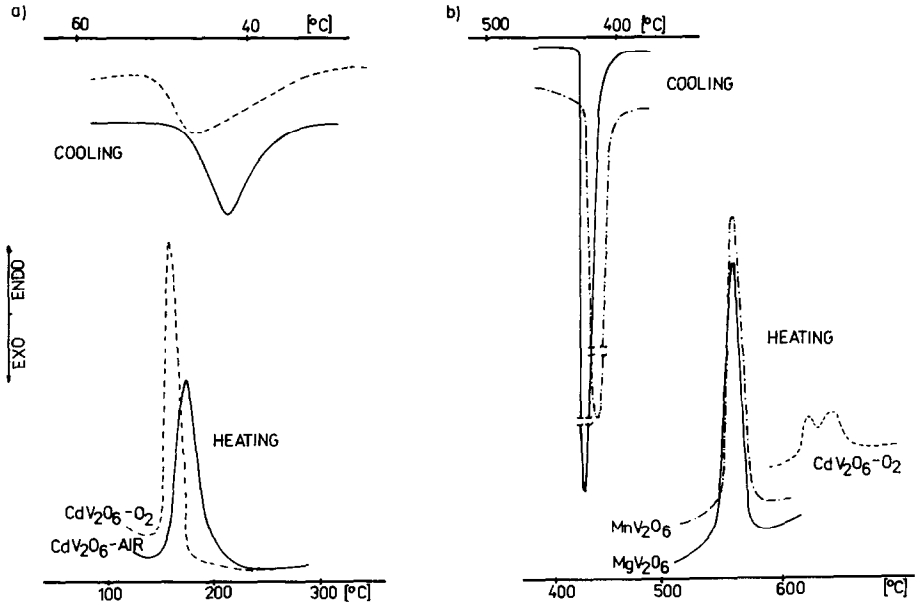


FIG. 2. DTA of $CdV_2O_6$ (in air and in oxygen), $MgV_2O_6$, and $MnV_2O_6$ (in air).

TABLE II

X-RAY POWDER DIFFRACTION DATA FOR $MgV_2O_6$-B AT ROOM TEMPERATURE

| *hkl* | $d_{obs}$ (Å) | $d_{cal}$ (Å) | $I_{obs}$ | *hkl* | $d_{obs}$ (Å) | $d_{cal}$ (Å) | $I_{obs}$ |
|---|---|---|---|---|---|---|---|
| 001 | 6.25 | 6.25 | s | $11\bar{3}$ | 1.875 | 1.875 | w |
| $20\bar{1}$ | 4.39 | 4.39 | w | 401 | 1.839 | 1.839 | w |
| 200 | 4.316 | 4.312 | s | 020 | 1.746 | 1.746 | w |
| 110 | 3.236 | 3.236 | m | $20\bar{4}$ | 1.683 | 1.683 | w |
| $20\bar{2}$ | 3.146 | 3.144 | s | 021 | | 1.681 | |
| 201 | 3.059 | 3.059 | vs | 203 | 1.651 | 1.652 | |
| $11\bar{1}$ | | 3.052 | | 113 | | 1.651 | |
| 111 | 2.724 | 2.723 | m | 312 | 1.605 | 1.606 | w |
| $40\bar{1}$ | 2.320 | 2.320 | vw | 510 | 1.546 | 1.546 | w |
| $31\bar{1}$ | 2.310 | 2.310 | w | $60\bar{2}$ | 1.540 | 1.540 | w |
| 310 | 2.219 | 2.219 | w | 402 | 1.529 | 1.530 | m |
| $40\bar{2}$ | 2.195 | 2.195 | m | $22\bar{2}$ | | 1.526 | |
| 202 | 2.177 | 2.177 | s | 022 | 1.525 | 1.524 | vw |
| 400 | 2.156 | 2.156 | w | 221 | 1.516 | 1.516 | vw |
| 112 | 2.107 | 2.107 | w | $51\bar{3}$ | 1.504 | 1.504 | w |
| 003 | 2.084 | 2.084 | m | $31\bar{4}$ | 1.495 | 1.495 | w |
| 311 | 1.925 | 1.925 | w | $11\bar{4}$ | 1.491 | 1.491 | vw |
| $40\bar{3}$ | 1.888 | 1.888 | w | 600 | 1.437 | 1.437 | m |

we have $\Delta H > 0$ and $\Delta V > 0$, which implies $dp/dT > 0$. Therefore on increasing pressure the B → P transition is shifted from 170 to 460°C.

*(ii)* $MgV_2O_6$

Our $MgV_2O_6$ preparation, synthesized as described under Experimental, had B-type structure at room temperature. As the indexed powder X-ray pattern has never been published, we give it in Table II. DTA of $MgV_2O_6$-B showed below the melting point (765°C) only one, narrow, endothermal peak at 558°C which was reversible on cooling with a hysteresis (Fig. 2b). High-temperature X-ray investigations (performed in the analogous way as for $CdV_2O_6$) prove that if the sample is left at elevated temperatures for a few scores of minutes to reach equilibrium, the B → P phase transformation is completed at 535°C. The product was found to have the P-type structure, stable till the melting point. The indexed pattern of $MgV_2O_6$-P at 560°C is given in Table III. The determined unit cell parameters for $MgV_2O_6$-B (at 26 and 525°C) and for $MgV_2O_6$-P (at 560°C) are gathered in Table IV.

*(iii)* $MnV_2O_6$

In agreement with the former reports (*1*, *5*, *19*), $MnV_2O_6$ is found to have B-type structure at room temperature. Its behavior on heating, followed with DTA and high-temperature X-ray analysis, was highly analogous to that of $MgV_2O_6$. A narrow, endothermal peak was observed in DTA at 564°C (on heating) which was reversible on cooling with a hysteresis (Fig. 2). Isothermally followed transition temperature (high-temperature X-ray camera) was found to be 540°C. High-temperature modification of $MnV_2O_6$ has been identified as $MnV_2O_6$-P. The determined structural data are included in Tables III and IV.

Concerning the B → P phase transformations taking place on heating of $CdV_2O_6$, $MgV_2O_6$, and $MnV_2O_6$, it seems of interest

TABLE III

X-RAY POWDER DIFFRACTION DATA FOR $MgV_2O_6$-P AND $MnV_2O_6$-P

| $MgV_2O_6$-P at 560°C | | | | $MnV_2O_6$-P at 600°C | | | |
|---|---|---|---|---|---|---|---|
| *hkl* | $d_{obs}$ (Å) | $d_{cal}$ (Å) | $I_{obs}$ | *hkl* | $d_{obs}$ (Å) | $d_{cal}$ (Å) | $I_{obs}$ |
| | | | | 001 | 6.72 | 6.74 | w |
| 200 | 4.74 | 4.74 | s | 200 | 4.77 | 4.77 | m |
| $20\bar{1}$ | 4.327 | 4.325 | m | $20\bar{1}$ | 4.374 | 4.375 | s |
| 201 | 3.526 | 3.529 | vs | 201 | 3.544 | 3.543 | vs |
| 110 | 3.345 | 3.344 | m | 002 | 3.366 | 3.369 | m |
| $11\bar{1}$ | 3.086 | 3.086 | m | 110 | | 3.366 | |
| $20\bar{2}$ | 3.058 | 3.058 | m | $11\bar{1}$ | 3.109 | 3.109 | m |
| 111 | 2.905 | 2.906 | m | $20\bar{2}$ | 3.094 | 3.092 | s |
| $40\bar{1}$ | 2.399 | 2.399 | w | 111 | 2.921 | 2.922 | s |
| 400 | 2.368 | 2.368 | m | 202 | 2.506 | 2.504 | vw |
| 310 | | 2.366 | | $40\bar{1}$ | 2.423 | 2.423 | vw |
| $31\bar{1}$ | 2.352 | 2.352 | vw | 400 | 2.385 | 2.386 | m |
| 003 | 2.232 | 2.232 | w | $31\bar{1}$ | 2.373 | 2.373 | m |
| 311 | 2.127 | 2.127 | w | 003 | 2.246 | 2.246 | m |
| 401 | 2.097 | 2.097 | w | 311 | 2.319 | 2.318 | m |
| $11\bar{3}$ | 1.925 | 1.925 | w | $11\bar{3}$ | 1.939 | 1.939 | m |
| 203 | 1.872 | 1.872 | w | 203 | 1.879 | 1.879 | w |
| $40\bar{3}$ | 1.830 | 1.830 | m | $40\bar{3}$ | 1.851 | 1.851 | m |
| 312 | 1.802 | 1.802 | m | 312 | 1.809 | 1.809 | m |
| 020 | 1.787 | 1.787 | w | 113 | | 1.805 | |
| | | | | 020 | 1.799 | 1.799 | m |
| | | | | 402 | 1.773 | 1.772 | vw |
| | | | | $20\bar{4}$ | 1.711 | 1.711 | w |
| | | | | 510 | 1.685 | 1.686 | vw |
| | | | | 004 | | 1.685 | |
| | | | | 220 | | 1.883 | |
| | | | | $22\bar{1}$ | 1.664 | 1.664 | vw |
| | | | | $51\bar{2}$ | 1.641 | 1.641 | w |

to stress that the relative differences between the lattice parameters of B and P forms ($\Delta p\%$) are practically the same for all three studied compounds (cf. Tables I and III).

*(iv)* $ZnV_2O_6$

In a separate paper (*17*) we intend to describe the synthesis and properties of the solid solutions of $MoO_3$ and $Li_2O$ in $ZnV_2O_6$. The quoted paper will also include some data for pure $ZnV_2O_6$. Here we would like to mention that, according to our studies and in agreement with the literature, the only modification that is stable between room temperature and the melting points is $ZnV_2O_6$-B.

## Conclusions

It has been proved that $CdV_2O_6$, $MgV_2O_6$, and $MnV_2O_6$ crystallize at normal pressure in two modifications, the low-temperature from being of the brannerite-type structure and the high-temperature form of pseudobrannerite-type structure. The transition temperatures are 170, 535, and 540°C, respectively, for Cd-, Mg-, and Mn-containing metavanadates. Phase transition in each case is followed by the increase of the

TABLE IV

UNIT CELL DIMENSIONS FOR B- AND P-MODIFICATIONS OF $MgV_2O_6$ AND $MnV_2O_6$[a]

| | $MgV_2O_6$-B | | $MgV_2O_6$-P | $p$ (%)[b] | $MnV_2O_6$-B | | $MnV_2O_6$-P | $p$ (%)[c] |
|---|---|---|---|---|---|---|---|---|
| $T$ (°C) | 26 | 525 | 560 | | 24 | 535 | 600 | |
| $a$ (Å) | 9.284(1)[d] | 9.378(2) | 9.695(3) | 3.4 | 9.310(3) | 9.396(3) | 9.783(3) | 4.1 |
| $b$ (Å) | 3.491(1) | 3.497(1) | 3.5735(10) | 2.2 | 3.5345(12) | 3.542(1) | 3.598(1) | 1.6 |
| $c$ (Å) | 6.731(1) | 6.798(3) | 6.854(2) | 0.8 | 6.753(2) | 6.816(2) | 6.908(2) | 1.3 |
| $\beta$ (deg) | 111.74(1) | 110.37(1) | 102.29(1) | −7.3 | 112.58(1) | 111.43(2) | 102.73(1) | −7.8 |
| $c \sin \beta$ (Å) | 6.252(1) | 6.373(3) | 6.697(2) | 5.1 | 6.235(2) | 6.345(3) | 6.738(2) | 3.9 |
| $V$ (Å$^3$) | 202.63 | 208.99 | 232.03 | 11.0 | 205.19 | 211.19 | 237.18 | 12.3 |
| $Z$ | 2 | 2 | 2 | | 2 | 2 | 2 | |

[a] Systematic absences of reflections $h + k = 2n + 1$ were observed for all compounds and temperatures.

[b] $\Delta p = \frac{p_{560} - p_{525}}{p_{525}} \times 100$ (cf. Table I).

[c] $\Delta p = \frac{p_{500} - p_{535}}{p_{535}} \times 100$ (cf. Table I).

[d] Estimated standard deviation in parentheses.

unit cell volume by about 11–12%. These data combined with the results of our former studies and with literature data make it possible to construct a consistent scheme of the phase transformations of the $MeV_2O_6$ compounds, which is shown in Fig. 3. Figure 3 makes it possible to conclude that among the considered $MeV_2O_6$

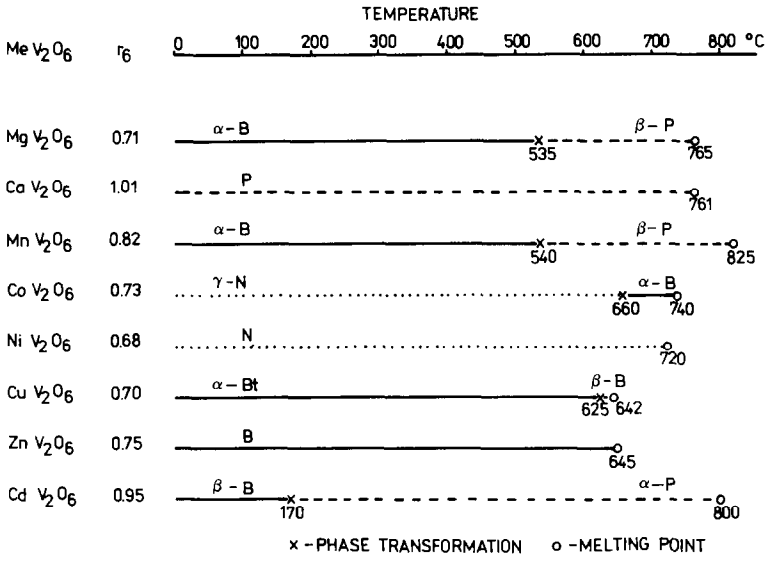


FIG. 3. Scheme of the phase transformations of the $MeV_2O_6$ metavanadates at normal pressure between room temperature and melting points. B = Brannerite type, P = pseudobrannerite type, and N = $NiV_2O_6$-type structures; Bt means B with a little triclinic distortion; $\alpha$, $\beta$, and $\gamma$ are the traditional symbols of polymorphs used so far in the literature. Ionic radii $r_6$ (27) of $Me^{2+}$ in octahedral coordination are indicated, which have an influence on the structure type (see text).

compounds, brannerite-type structure is the most common one. At higher temperatures some of the $MeV_2O_6$ compounds (*Me* = Mg, Mn, Cd) adopt the pseudobrannerite-type structure of a lower density. B → P transformation seems to be favored by an increase of the cation size, so that the largest *Me* = Ca (of the ionic radius in octahedral coordination $r_6$ = 1.01 Å (*27*)) forces the structure to be of P-type in the entire temperature range. For the next largest, *Me* = Cd ($r_6$ = 0.95 Å), the temperature of transformation is 170°C only, while for smaller *Me* = Mn, Mg the B → P transition takes place above 500°C. It seems appropriate to note that although the ionic radius of $Mg^{2+}$ in octahedral coordination is $r_6$ = 0.71 Å (*27*), it behaves in the B-type structure as if it was 0.78 Å (average Mg–O distance in $MgV_2O_6$ (*4*)). The behavior of $Mg^{2+}$ will be considered again below. On the other hand, for small cations of $r_6 \approx 0.7$ Å and of a peculiar *d*-shell structure, either triclinic distortion Bt is observed ($Cu^{2+}$, $d^9$) or N-type structure appears, being a unique form for $NiV_2O_6$ ($Ni^{2+}$, $d^8$) or a low-temperature modification for $CoV_2O_6$ ($Co^{2+}$, $d^7$). The above-formulated dependence of the structure of the $MeV_2O_6$ compounds on *Me* size is an extension of some observations already formulated in the literature (*18*). It may be of interest to add after (*18*) that $MeV_2O_6$ compounds containing very large *Me* cations (Sr, Ba, Pb, Hg), not considered in this work, crystallize in orthorhombic structures.

In view of the above-formulated dependence of the structure on the size of $Me^{2+}$ cations it seems of interest to compare the lattice parameters (Table V) and some interatomic distances (Table VI) in the structures under consideration.

As already mentioned in the Introduction, the anionic layers in the brannerite-type structure, parallel to (001), may be considered to be composed of zigzag $(VO_6)_n$ chains extending along (010) and linked to one another by the edges. Independently of *Me*, the bond lengths in $VO_6$ octahedra (cf. Table VI) may be simplified as 2 × 1.68, 2 × 1.85, 1 × 2.10, and 1 × ~2.6 Å. Typical $O_1$–$O_1$ and $O_1$–$O_2$ distances are ~3.5 and ~3.0 Å, where $O_1$–$O_1$ means the distance between oxygens protruding from corner-sharing octahedra along the zigzag chain and $O_1$–$O_2$ the same for edge-sharing octahedra. It is striking that similar zigzag chains exist in the structure of $V_2O_5$ (*28*) (cf. Table VI) with sizes very close to the above-indicated set. This means that the structure of the anionic layer in brannerites is rather rigid and ruled by properties of the vanadium cation. This is a rather expected observation as the av-

TABLE V

LATTICE PARAMETERS OF $MeV_2O_6$ COMPOUNDS OF BRANNERITE- (B) AND PSEUDOBRANNERITE- (P) TYPE STRUCTURES AS RELATED TO THE IONIC RADII OF *Me*

| | | $MeV_2O_6$-B | | | | | $MeV_2O_6$-P | | | | | |
|---|---|---|---|---|---|---|---|---|---|---|---|---|
| *Me* | $r_6$ (Å) | *a* (Å) | *b* (Å) | *c* (Å) | β (deg) | *V* (Å³) | *a* (Å) | *b* (Å) | *c* (Å) | β (deg) | *V* (Å³) | Reference |
| Mg | 0.71 | 9.284 | 3.491 | 6.731 | 111.74 | 202.6 | 9.695 | 3.573 | 6.854 | 102.29 | 232.0 | This work 560°C |
| Co | 0.73 | 9.251 | 3.504 | 6.618 | 111.64 | 199.4 | — | — | — | — | — | (*7*) |
| Zn | 0.75 | 9.240 | 3.528 | 6.571 | 111.36 | 199.5 | — | — | — | — | — | (*17*) |
| Mn | 0.82 | 9.310 | 3.534 | 6.753 | 112.58 | 205.2 | 9.783 | 3.598 | 6.908 | 102.73 | 237.2 | This work 600°C |
| Cd | 0.92 | 9.363 | 3.566 | 6.950 | 112.13 | 214.9 | 9.837 | 3.618 | 7.020 | 103.58 | 242.5 | This work 250°C |
| Ca | 1.01 | — | — | — | — | — | 10.060 | 3.673 | 7.038 | 104.8 | 251.4 | (*13*) |

TABLE VI

INTERATOMIC DISTANCES IN $V_2O_5$ AND $MeV_2O_6$ COMPOUNDS OF BRANNERITE- (B) AND PSEUDOBRANNERITE- (P) TYPE STRUCTURES AND BOND STRENGTH[a] SUMS AROUND *Me* AND V

| Distance[b] | $V_2O_5$ | $MgV_2O_6$-B | $ZnV_2O_6$-B | $CdV_2O_6$-B | $CdV_2O_6$-P | $CaV_2O_6$-P |
|---|---|---|---|---|---|---|
| $O_1$–$O_{1'}$ | — | 2.66 | 2.65 | 2.98 | 2.81 | 2.94 |
| $O_1$–$O_1$ | 3.56 | 3.49 | 3.53 | 3.57 | 3.62 | 3.67 |
| $O_1$–$O_2$ | 2.99 | 2.97 | 3.00<br>2.89 | 3.12 | 3.07 | 3.37 |
| $O_1$–$O_{2'}$ | — | 3.00 | 3.04<br>2.93 | 3.29 | 3.27 | 3.27 |
| *Me*–$O_1$ 4× | — | 2.19 | 2.35<br>2.06 | 2.32 | 2.29 | 2.35 |
| *Me*–$O_2$ 2× | — | 2.02 | 1.99 | 2.21 | 2.20 | 2.34 |
| V–$O_1$ | 1.58 | 1.67 | 1.70 | 1.68 | 1.68 | 1.68 |
| V–$O_2$ | 1.78 | 1.67 | 1.68 | 1.69 | 1.71 | 1.61 |
| V–$O_2$ | 2.78 | 2.67 | 2.54 | 2.46 | 3.57 | 3.67 |
| V–$O_3$ 2× | 1.88 | 1.85 | 1.83 | 1.87 | 1.88 | 1.90 |
| V–$O_3$ | 2.02 | 2.11 | 2.10 | 2.09 | 1.98 | 1.97 |
| $\Sigma s_{V-O}$ | 5.00 | 4.88 | 4.83 | 4.76 | 4.59 | 5.00 |
| $\Sigma s_{Me-O}$ | — | 1.95 | 2.26 | 2.38 | 2.48 | 2.31 |

[a] Bond strength is calculated using a columbic-type formula (*27*).

[b] $O_1$–$O_1$ means the distance between oxygens protruding from corner-sharing octahedra along the zigzag chain and $O_1$–$O_2$ the same for edge-sharing octahedra. Oxygens belonging to the next anionic layer are distinguished with a prime.

erage strength of V–O bonds is $s_{V-O} = 0.83$ v.u., while that of *Me*–O bonds is $s_{Me-O} = 0.33$ v.u. only. $Me^{2+}$ cations are therefore forced to find the energetically most convenient sites between 2 × $O_1$ and $O_2$ of one layer and 2 × $O_1$ and $O_2$ of the next layer. All they may "wish for" is to what extent the layers are distant and slide along [100]; this is limited, however, by the repulsive forces between oxygens belonging to the neighboring layers. Only minor modifications of the $O_1$–$O_1$ and $O_1$–$O_2$ distances inside the layers are possible for $Me^{2+}$ to reach the convenient set of *Me*–O bond lengths. In the case of large $Cd^{2+}$, these distances are slightly increased; in the case of small $Mg^{2+}$ and $Zn^{2+}$, they are diminished as compared to those in $V_2O_5$, however, without changes in the length of V–O bonds.

B → P phase transformation in $CdV_2O_6$ results in the shortening of Cd–O bonds and in increasing their strength at the expense of V–O bonds (Table VI). This is due to the fact that the zigzag chains in P-type structure are isolated and turned around [010], so that $Cd^{2+}$ ions may have a better contact with $O_1$ and $O_2$. The sizes of $CdO_6$ and $VO_6$ octahedra do not change markedly on B → P transformation, but the unit cell volume increases by about 13% due to the appearance of empty channels between zigzag anionic chains. In contrast to $CdV_2O_6$, $Mg^{2+}$ in $MgV_2O_6$-B is too small to reach the required bond lengths. The rigidity of anionic layers allows for the shortening of $O_1$–$O_1$ and $O_1$–$O_2$ distances to 3.49 and 2.97 Å only. The layers may not be situated more compactly because of the repulsive forces ($O_1$–$O_{1'}$ is 2.66 Å, which is

close to the sum of the ionic radii of two $O^{2-}$). This is the reason why $Mg^{2+}$ in the brannerite-type matrix behaves as a cation of a size larger than expected. Apparently in P-type structure $Mg^{2+}$ finds better arrangement of oxygens around it (unfortunately the positions of atoms in $MgV_2O_6$-P are not known at present). It seems interesting to note that $Zn^{2+}$ in $ZnV_2O_6$-B (shifted to a tetrahedral-like position) reaches (among $Me^{2+}$) the best fit between its size and the size requirements of the anionic sheets. The shortest oxygen–oxygen distances are 2.65, 2.89, and 2.93 Å. The sum of the bond strengths around $Zn^{2+}$ is 2.26 v.u., being much higher than that around $Mg^{2+}$ (1.95 v.u.) in $MgV_2O_6$-B and close to those around $Cd^{2+}$ and $Ca^{2+}$ in all three structures of these cations. Therefore $ZnV_2O_6$-B "is apparently not interested" in transforming into a P-type form: $\Sigma s$ around $Zn^{2+}$ is high enough and oxygen–oxygen repulsive forces even prevent further shortening of Zn–O and O–O distances.

The changes of the unit cell volume with ionic radius of $Me^{2+}$ (Table V) speak in favor of the above interpretation. For larger cations ($Cd^{2+}$, $Mn^{2+}$, $Zn^{2+}$) the volume decreases with a decrease of cation size, but for the next smaller cation, $Co^{2+}$, this decrease is stopped and for $Mg^{2+}$ the unit cell volume increases again. Analogous observations can be made for other lattice parameters. Similar exceptional behavior of $Mg^{2+}$ has already been observed in $MeV_2O_6$ and $MeNb_2O_6$ compounds of brannerite and columbite structures (*1*) and attributed to the relatively greater covalence and consequent shortening of *Me*–O bonds, where *Me* = Ni, Co, Zn, Mn, Cd. This is a rather surprising conclusion as covalent bonds are expected to be longer compared to the ionic ones: first, this is predicted by the Schomaker–Stevenson rule (*29*) and, second, the sums of covalent radii of oxygen and metal (*30*) are larger compared to the sums of the respective ionic radii (*27, 31*). Therefore we believe that the oxygen–oxygen repulsive forces should be responsible for the exceptional behavior of $Mg^{2+}$. The same phenomenon could be expected for compounds of other small ions ($Ni^{2+}$, $Cu^{2+}$, and possibly $Co^{2+}$) if they formed B-type structures at room temperature. However, these compounds adapt other structures in which, apparently, stronger *Me*–O bonds are possible. $Cu^{2+}(d^9)$ reaches its stabilization because of the Jahn–Teller effect, resulting in triclinic distortion of the brannerite-type structure. $Co^{2+}(d^7)$ and $Ni^{2+}(d^8)$, for which the Jahn–Teller effect is expected to be either weaker or absent, choose another N-type structure.

To make the above explanation more profound, the knowledge of the N-type structure and reexamination of the space groups of B- and P-type phases (especially for $MgV_2O_6$) would be highly desirable.

## Acknowledgment

The authors thank Dr. Agnieszka Pattek from the Jagiellonian University (Kraków) for her kind assistance with the measurements of crystal density.

## References

1. M. Gondrand, A. Collomb, J. C. Joubert, and R. D. Shannon, *J. Solid State Chem.* **11,** 1 (1974).
2. D. Mercurio, J. Galy, and B. Frit, *C.R. Acad. Sci. Paris C* **282,** 27 (1976).
3. T. Machej, R. Kozłowski, and J. Ziółowski, *J. Solid State Chem.* **38,** 97 (1981).
4. H. N. Ng and C. Calvo, *Canad. J. Chem.* **50,** 3619 (1972).
5. R. Kozłowski, J. Ziółkowski, K. Mocała, and J. Haber, *J. Solid State Chem.* **35,** 1 (1980); erratum **38,** 138 (1981).
6. E. E. Sauerbrei, M. Sc. thesis, McMaster University, Hamilton, Ontario, Canada (1972).
7. K. Mocała, J. Ziółkowski, and L. Dziembaj, *J. Solid State Chem.* **56,** 84 (1985).
8. C. Calvo and D. Manolescu, *Acta Crystallogr., Sect. B* **29,** 1743 (1973).
9. J. Angenault, *Rev. Chim. Miner.* **7,** 651 (1970).

10. J. ANGENAULT, AND A. RIMSKY, *C.R. Acad. Sci. Paris* **267,** 227 (1968).
11. J. C. BOULOUX AND J. GALY, *Bull. Soc. Chim. Fr.* **3,** 736 (1969).
12. R. RUH AND A. D. WADSLEY, *Acta Crystallogr.* **21,** 974 (1966).
13. J. C. BOULOUX, P. PEREZ, AND J. GALY, *Bull. Soc. Fr. Mineral. Crystallogr.* **95,** 130 (1972).
14. G. PEREZ, B. FRIT, J. C. BOULOUX, AND J. GALY, *C.R. Acad. Sci. Paris C* **270,** 952 (1970).
15. C. BRISI, *Ann. Chim.* **47,** 806 (1957).
16. G. M. CLARK AND A. N. PICK, *J. Thermal Anal.* **7,** 289 (1975).
17. K. MOCAŁA AND J. ZIÓŁKOWSKI, *J. Solid State Chem.* **69,** 299 (1987).
18. P. GARNIER AND D. WEIGEL, *J. Solid State Chem.* **47,** 16 (1983).
19. J. ZIÓŁKOWSKI, K. KRUPA, AND K. MOCAŁA, *J. Solid State Chem.* **48,** 376 (1983).
20. G. GARCIA-CLAVEL, S. GOÑI-ELIZALDE, AND S. FRESNO-RUIZ, *in* "Proceedings, 10th International Symposium on Reactivity of Solids, Dijon 1984" (P. Barret and L. C. Dufour, Eds.), p. 599, Elsevier, Amsterdam/New York (1985).
21. G. GARCIA-CLAVEL, S. GOÑI-ELIZALDE, AND S. FRESNO-RUIZ, *in* "Proceedings, 8th International Conference on Thermal Analysis, Bratislava, 1985" *Thermochim. Acta* **95,** 501 (1985).
22. A. MATTHEWS, *Amer. Mineral.* **61,** 419 (1976).
23. G. M. CLARK AND R. MORLEY, *J. Solid State Chem.* **16,** 429 (1976).
24. B. W. Slobodin, N. G. Sharova, and T. I. Krasnenko, *Izv. Akad. Nauk SSSR, Neorg. Mater.* **20,** 688 (1984).
25. O. G. PALANNA, *Proc. Indian Acad. Sci. A* **88,** Part 1, 19 (1979).
26. Z. KLUZ AND I. WACŁAWSKA, *Polish J. Chem. (Rocz. Chem.)* **49,** 839 (1975).
27. J. ZIÓŁKOWSKI, *J. Solid State Chem.* **57,** 269 (1985).
28. H. G. BACHMAN, F. R. AHMED, AND W. H. BARNES, *Z. Kristallogr.* **115,** 110 (1961).
29. V. SCHOMAKER AND D. P. STEVENSON, *J. Amer. Chem. Soc.* **63,** 37 (1941).
30. R. T. SANDERSON, "Chemical Periodicity," Reinhold, New York (1962).
31. R. D. SHANNON, *Acta Crystallogr., Sect. A* **32,** 751 (1976).